A Study on the Interfacial exchange coupling in the FMR setup on a FI-2DHG junction.

M.Sc. Thesis

M.Sc. Physics

Indian Institute of Technology Indore



Author: Deepak Kumar

Roll No: 2303151010

Supervisor: Dr. Alestin Mawrie

Indian Institute of Technology Indore

May 12, 2025

A Study on the Interfacial exchange coupling in the FMR setup on a FI-2DHG junction.

A THESIS

Submitted in partial fulfillment of the requirements for the award of the degree

of

Master of Science

by

DEEPAK KUMAR



DISCIPLINE OF Msc Physics

INDIAN INSTITUTE OF TECHNOLOGY INDORE

May 2025



INDIAN INSTITUTE OF TECHNOLOGY INDORE

CANDIDATE'S DECLARATION

I hereby certify that the work which is being presented in the thesis entitled A

Study on the Interfacial exchange coupling in the FMR setup on a

FI-2DHG junction. in the partial fulfillment of the requirements for the award of the degree of MASTER OF SCIENCE and submitted in the

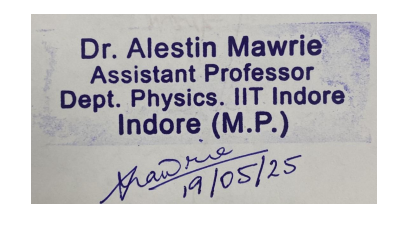
DISCIPLINE OF Physics, Indian Institute of Technology Indore, is an authentic record of my work carried out during the time period from July 2023 to May 2025 under the supervision of Dr. Alestin Mawrie.

The matter presented in this thesis has not been submitted by me for the award of any other degree of this or any other institute.

Deepak 19/05/25

Signature of Student: Deepak Kumar

This is to certify that the above statement made by the candidate is correct to the best of my/our knowledge.



Signature of the Supervisor of

M.Sc. thesis (with date)

(Dr. Alestin Mawrie)

21-05-25
Signature of the DPGC convener
(with date)

DEEPAK KUMAR has successfully given his/her M.Sc. Oral Examination held on May 13, 2025.

Acknowledgement

I would like to sincerely thank my supervisor, Dr. Alestin Mawrie and my senior, Sushmita Saha, for their patience, constant guidance, and for answering my endless questions. Their support extended far beyond this thesis, helping me grow both academically and in pursuit of my chosen career path. To my friends, thanks for those much-needed lunch and tea breaks that made even the most stressful moments enjoyable and memorable. I am also grateful to my college, the Indian Institute of Technology Indore, for providing not just a beautiful campus and excellent facilities, but also the Learning Resource Centre and a nurturing environment that has helped shape a mindset of continuous growth. Lastly, to everyone who supported and cheered me on — knowingly or unknowingly — thank you. This thesis is as much yours as it is mine.

Contents

Contents				
Abbreviations List of Figures				
2	For	mulation	7	
	2.1	Two-Dimensional Electron Gas	7	
	2.2	Ferromagnetic Insulator	8	
	2.3	Interfacial exchange interaction	9	
	2.4	Second-order perturbation	9	
	2.5	Results of 2-Dimensional Electron Gas	11	
3	Spin	n pumping via a 2D Heavy Hole Gas	15	
	3.1	2DHG's Introduction	16	
	3.2	Composite system Hamiltonian	18	
	3.3	Two-Dimensional Heavy Hole Gas	18	
	3.4	Ferromagnetic Insulator	21	
	3.5	Interfacial Exchange Interaction	23	
	3.6	Gilbert Damping Calculation	23	
	3.7	Result of 2D Heavy Hole Gas	25	
	3.8	Enhancement of Gilbert Damping	27	

4 Summary	30
Bibliography	32

Abstract

In this project, we study spin pumping using ferromagnetic irradiation in a junction of ferromagnetic insulator and a 2D hole gas of a p-AlGaAs/GaAs semiconductor heterostructure. We use microwave radiation to precess the spin in the ferromagnetic insulator layer. In a 2-dimensional hole gas, the Rashba SOC and Dresselhaus SOC interactions coexist and play crucial roles in our spin pumping system by delivering two spin species electrons, spin-up and spin-down, which in turn interact with the spins from the ferromagnetic layer. We then calculate the interfacial exchange coupling by using second-order perturbation theory, which helps us deduce an increment in the spectral width of the Gilbert damping factor. We show the increment in Gilbert damping to the spin orientations in the ferromagnetic insulator, induced through their interactions with the spin species from the 2D Hole Gas.

Abbreviations

2DEG Two Dimensional Electron Gas

2DHG Two Dimensional Hole Gas

FI Ferromagnetic Insulator

RSOC Rashba Spin Orbit Coupling

SOC Spin-Orbit Coupling

FMR Ferromagnetic Resonance

SIA Structural Inversion Symmetry

STT Spin Transfer Torque

GD Gilbert Damping

List of Figures

1.1	A schematic of the junction between the F1 and the 2D electron	
	gas in a semiconductor heterostructure.[1]	5
1.2	Band diagram of 2DHG formed at junction of AlGaAs and GaAs	6
2.1	A schematic picture of the fixed frame of reference and rotated	
	coordinate frame of reference	9
2.2	Diagram of the effective magnetic field $\operatorname{heff}(\phi)$ acting on the car-	
	rier electrons' spin when both the coefficients have a ratio of 1	
	and 3	12
2.3	The increment in Gilbert damping, $\delta \alpha_G$ in 2DEG with FMR reso-	
	nance frequency for $\frac{\alpha}{\beta} = 1$	13
2.4	The increment in Gilbert damping, $\delta \alpha_G$ in 2DEG with FMR reso-	
	nance frequency for $\frac{\alpha}{\beta} = 3$	13
2.5	The contour plot for frequency vs Gilbert Damping	14
3.1	Schematic of our system with a ferromagnetic layer irradiated	
	with microwave frequency, in junction with 2DHG in semiconduc-	
	tor heterostructure	17

3.2	Energy dispersion $E_s(k)$ due to SOC, in which the pink part rep-	
	resents the $s=+1$ and the other colour represents to $s=-1$.	
	Arrows represent the spin configuration along the Fermi contours,	
	which shows the opposing chirality of the two parts. The parame-	
	ters are chosen such that the ratio of spin-orbit coupling strengths	
	is $\alpha/\beta=2$	20
3.3	variation in the δ with frequencies \mathbf{k}	26
3.4	Schematic of contour plot at range of frequecies frequencies δ	27
3.5	The curve showing enhancement of Gilbert damping vs frequency	
	at different values of Rashba coefficient α	28

Chapter 1

Introduction

In Spintronics, spin pumping is widely studied as a resourceful method for spin current generation using magnetisation dynamics. This process typically involves using ferromagnetic materials in which precession of magnetisation induces a spin current into an adjacent normal metal. This is achieved by exciting the magnetisation in the FI layer, often through FMR, which transfers the angular momentum to the electrons in the adjacent layer. The angular momentum transfer in spin pumping occurs through the dynamic exchange interaction at the interface between the ferromagnetic and other materials. This interaction effectively "pumps" spin angular momentum from the ferromagnetic Insulator into the adjacent non-magnetic layer. The transferred angular momentum shows clearly as a spin current. Exchange interaction refers to an effect responsible for the alignment of spins in ferromagnetic materials. It is a fundamental interaction between the spins of neighbouring electrons. Electrons tend to arrange themselves to minimise the total energy of the system. In FI, it often leads to the parallel alignment of neighbouring electron spins because such an arrangement minimises the repulsive coulomb energy when the spatial part of the function overlaps.

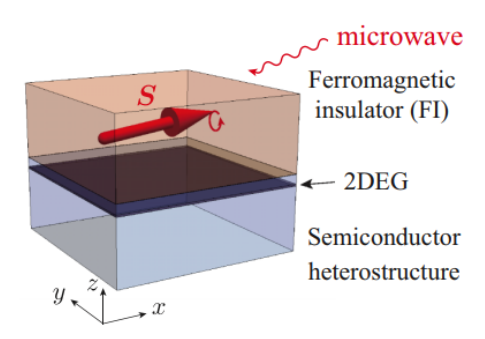


Figure 1.1: A schematic of the junction between the FI and the 2D electron gas in a semiconductor heterostructure.[1]

In SOC, the spin of the electron, which is its intrinsic angular momentum, becomes linked to its orbital angular momentum. It means that the spin orientation of electrons can affect the electrons' orbital motion and vice versa. The strength of this interaction depends on the atomic number of the atom(heavier atoms have stronger SOC). Rashba is a special type of SOC that occurs in systems with SIA, such as at the Interface, coupling because intrinsic and orbital angular momentum are interlinked. Initially, most studies focused on spin current injection into a 2DEG. However, in recent years, the focus has shifted toward 2DHG. 2DHG occurring in p-type AlGaAs/GaAs heterostructures, where the SIA-induced SOC exhibits a cubic dependence on momentum due to the p-orbital nature of holes, unlike 2DEG, where the dependency is linear. This leads to cubic Rashba SOC, resulting in stronger spin—orbit interaction. The larger effective mass of heavy holes and their higher density of states at the Fermi level enhance their interaction with the magnetic system, which makes our 2DHG a promising system for more efficient spin absorption.

This thesis is further organised as follows:

In Chapter 2, we establish the theoretical framework by introducing the Hamiltonians for the 2DEG, FI, and their interfacial interaction. We used Green's function method and second-order perturbation theory to calculate self-energy corrections and Gilbert damping. These formulations are later applied to the

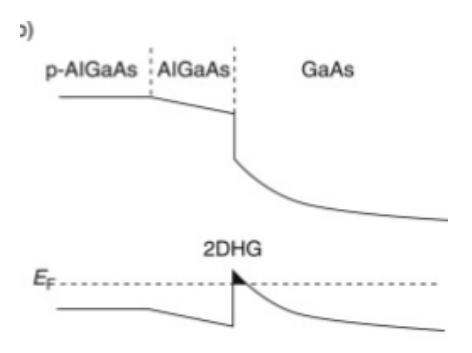


Figure 1.2: Band diagram of 2DHG formed at junction of AlGaAs and GaAs.

2DHG system.

In chapter 3, we focus on the same spin pumping framework in a 2DHG. The SOC in 2DHG is cubic in momentum due to the p-orbital nature of holes, making the spin dynamics more intricate. Our focus is on understanding how interband transitions and enhanced SOC in 2DHG influence Gilbert damping more strongly.

We conclude this M.Sc. thesis in Chapter 4 by summarising the key results obtained from both 2DEG and 2DHG systems.

Chapter 2

Formulation

2.1 Two-Dimensional Electron Gas

The Hamiltonian of the 2DEG in n-doped AlGaAs/GaAs heterojunction is written as

$$H_{\rm kin} = \sum_{k} \left(c_{k\uparrow}^{\dagger} \ c_{k\downarrow}^{\dagger} \right) \hat{h}_{k} \begin{pmatrix} c_{k\uparrow} \\ c_{k\downarrow} \end{pmatrix}. \tag{2.1}$$

where \hat{h}_k is the Hamiltonian matrix, expressed as[1]:

$$\hat{h}_k = \left(\frac{\hbar^2 (k_x^2 + k_y^2)}{2m^*} - \mu\right) \mathbb{I} + \alpha (k_y \sigma_x - k_x \sigma_y) + \beta (k_x \sigma_x - k_y \sigma_y).$$

We have the Hamiltonian of a 2DEG, which we will use in getting the information out of the 2DEG while injecting the spins from a ferromagnetic insulator. The increase in the Rashba coefficient increases the effective magnetic field acting on the spins, alters the spin pumping effect, and increases the energy dissipation in the ferromagnetic insulator. This causes a high damping value. Given the Hamiltonian, we can reduce it to

$$\hat{h}_k = \xi \mathbb{I} - \hat{h}_{ ext{eff}} \cdot \boldsymbol{\sigma}$$

which can be used frequently. This is just the reduced form of the above Hamiltonian. $h_{\text{eff}}(\varphi) \equiv |h_{\text{eff}}(\varphi)| \simeq k_F \sqrt{\alpha^2 + \beta^2 + 2\alpha\beta\sin(2\varphi)}$. The above is the effective magnetic field due to atoms.

$$\hat{g}(k, i\omega_n) = \frac{(i\hbar\omega_n - \xi_k)\mathbb{I} - \mathbf{h}_{\text{eff}} \cdot \boldsymbol{\sigma}}{(i\hbar\omega_n - E_k^+)(i\hbar\omega_n - E_k^-)}$$

. This is the calculated Green's function for the Hamiltonian, We also look for impurity effects in it, which is then given by

$$\hat{g}(k, i\omega_n) = \frac{[i\hbar\omega_n - \xi_k + i\frac{\Gamma}{2}\mathrm{sgn}(\omega_n)]\hat{I} - \hat{h}_{\mathrm{eff}} \cdot \boldsymbol{\sigma}}{\prod_{\nu=\pm} \left[i\hbar\omega_n - E_{k\nu} + i\frac{\Gamma}{2}\mathrm{sgn}(\omega_n - E_{k\nu} + i\frac{\Gamma}{2}\mathrm{sgn}(\omega_n) \right]}$$

The impurities are mainly due to scattering. Now we will come to our next part of the material, which is the ferromagnetic insulator.

2.2 Ferromagnetic Insulator

In this ferromagnetic insulator, we will work on the rotated coordinate system, Now, assuming that the net magnetic moment of the ferromagnetic insulator is in the x-y plane, which is parallel to the 2DEG. The Hamiltonian of a ferromagnetic insulator is given by [1]

$$H_{FI} = \sum_{\langle i,j \rangle} J_{ij} \left(S_i^{x'} S_j^{x'} + S_i^{y'} S_j^{y'} + S_i^{z'} S_j^{z'} \right) - \hbar \gamma h_{dc} \sum_i S_i^{x'}$$

where J_{ij} is the exchange interaction of ferromagnetic material, γ (< 0) is the gyromagnetic ratio, $\langle i,j \rangle$ shows a pair of directly adjacent sites. The reduced form for this Hamiltonian can be given by $H_{FI} = \sum_k \hbar \omega_k b_k^{\dagger} b_k$

$$\hbar\omega_k = Dk^2 + \hbar\gamma h_{dc}$$

where b_k is the magnon's lowering operator and D is the stiffness of spin.

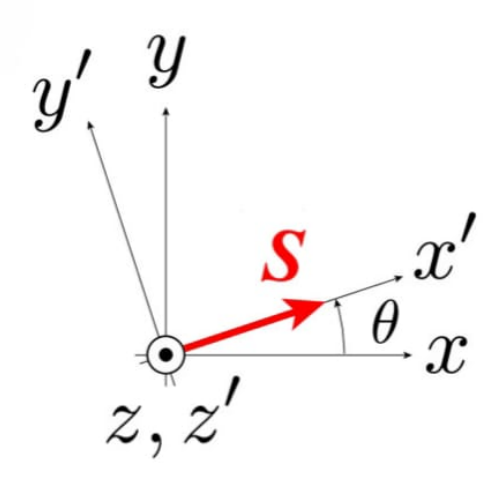


Figure 2.1: A schematic picture of the fixed frame of reference and rotated coordinate frame of reference.

2.3 Interfacial exchange interaction

For this, the Hamiltonian is given by $\mathcal{H}_{\text{int}} = \sum_{k} \left(T_{k} S_{x'}^{+} S_{x'}^{-} + T_{k}^{*} S_{k}^{x'-} S_{k}^{x'+} \right);$ here $S_{k}^{x'\pm} = S_{k}^{y'} \pm i S_{k}^{z'}$ are raising and lowering operators of the localised spins in FI. T_{k} is an exchange interaction at the interface.

2.4 Second-order perturbation

We assume some second-order perturbation due to the interplay between the ferromagnetic layer and 2DEG, causing some change and introducing self-energy terms created due to this interaction. We can write the spin correlation function as [1]

$$G(k, i\omega_n) = \frac{1}{(G_0(k, i\omega_n))^{-1} - \Sigma(k, i\omega_n)},$$

where the self-energy $\Sigma(k, i\omega_n)$ is written as [1]

$$\Sigma(k, i\omega_n) = \frac{|T_k|^2}{4\beta} \sum_{k', i\omega_m} \operatorname{Tr} \left[\hat{\sigma}^{x'-} \hat{g}(k', i\omega_m) \times \hat{\sigma}^{x'+} \hat{g}(k'+k, i\omega_m + i\omega_n) \right]$$

This sigma part shows the self-energy term, while the $G_0(k, i\omega_n)$ represents the unperturbed part. Our work will mainly emphasise the increment in the frequency line width due to the coupling between FI and 2DEG. By analytic calculations, the correction for Gilbert damping is given by

$$\alpha_{G,0} \sum_{\nu,\nu'=\pm 1} \int_0^{2\pi} \frac{d\phi}{2\pi} F\left[\hbar\Omega + (\nu - \nu')h_{\text{eff}}\right] \times \frac{1 - \nu \hat{h}_{\text{eff}}(\phi) \cdot \hat{m}}{2} \frac{1 + \nu' \hat{h}_{\text{eff}} \cdot \hat{m}}{2}$$

$$F(x) = \frac{\Gamma}{\pi \Delta_0} \cdot \frac{1}{\left(\frac{x}{\Delta_0}\right)^2 + \left(\frac{\Gamma}{\Delta_0}\right)^2}$$

Now we can get this equation reduced down to three important Gilbert Damping components that are

$$\delta\alpha G = \delta\alpha G_1 + \delta\alpha G_2 + \delta\alpha G_3$$

$$\delta\alpha G_1 = \alpha G_0 \int_0^{2\pi} \frac{d\phi}{2\pi} F(\hbar\Omega) \frac{1 - (\hat{h}_{\text{eff}} \cdot \hat{m})^2}{2}$$

$$\delta\alpha G_2 = \alpha G_0 \int_0^{2\pi} \frac{d\phi}{2\pi} F(\hbar\Omega - 2h_{\text{eff}}) (1 + \hat{h}_{\text{eff}} \cdot \hat{m})$$

$$\delta\alpha G_3 = \alpha G_0 \int_0^{2\pi} \frac{d\phi}{2\pi} F(\hbar\Omega + 2h_{\text{eff}}) (1 - \hat{h}_{\text{eff}} \cdot \hat{m})$$

We used these equations for plotting the curves of Gilbert damping with the frequency (Ω) in MATLAB.

Interpretation of the above expressions, the above expressions give us the taste or physical interpretation of the increment in the Gilbert damping factor. The first component $\delta \alpha G_1$ is from the elastic spin flip of conducting electrons that occurs due to the transversal component of the $H_{\rm eff}$ through the interfacial exchange interaction. In reality, $\delta \alpha G_1$ vanishes when $H_{\rm eff}$ is parallel or antiparallel

to the magnetic orientation of ferromagnetic insulator \hat{m} . Given the elastic nature of this process, the frequency-dependent component takes the form of a Lorentz function $F(\hbar\Omega)$, that has a maximum at $\omega=0$. The other contribution $\delta\alpha G_2$ comes from the spin wave absorption. It is a non-static process, as demonstrated by the displacement of the peak in the Lorentzian shape, the maximum of $F(\hbar\Omega-2h_{\rm eff})$ changes to $\Omega=\frac{2H_{\rm eff}(\phi)}{\hbar}$, at which the energy of magnon matches the spin-split energy gap of conduction electrons. This second component takes the highest value when the effective magnetic field is parallel to \hat{m} . It is congruent with the fact that the spin of a conduction electron transitions from a low-energy state $H_{\rm eff}$ to a higher state $-H_{\rm eff}$ by absorbing a spin carried by a magnon in the direction of $-\hat{m}$. It is worth noting that the second contribution disappears when $H_{\rm eff}$ is antiparallel to \hat{m} .

The last component, $\delta \alpha G_3$, arises from the spin wave emission process. This process is of no use in ferromagnetic resonance experiments because we take frequency Ω as positive.

2.5 Results of 2-Dimensional Electron Gas

We can write Gilbert damping as

$$\delta_{\alpha_G}(\omega) = \alpha_{G,0} \sum_{\nu,\nu'=\pm 1} \int_0^{2\pi} \frac{d\phi}{2\pi} F\left[\hbar\Omega + (\nu - \nu')h_{\text{eff}}\right] \times \frac{1 - \nu \hat{h}_{\text{eff}}(\phi) \cdot \hat{m}}{2} \frac{1 + \nu' \hat{h}_{\text{eff}} \cdot \hat{m}}{2}$$

Here $\alpha_{G,0}$ is the dimensionless parameter and $\delta_L(x) = \frac{\Gamma/2}{\pi x^2 + (\Gamma/2)^2}$ represents Lorentzian delta function. From $\alpha_{G,0}$, it is proof of the fact that the density of states plays an important part in defining the efficacy of the increased strength of the Gilbert damping. We investigate the influence of interfacial exchange on the Gilbert damping factor with numerical evaluations. We got the conclusion quantitatively on the impact of spin-flip scattering and SOC in increasing damping in the 2DEG.

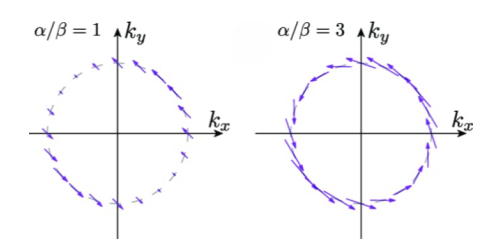


Figure 2.2: Diagram of the effective magnetic field heff(ϕ) acting on the carrier electrons' spin when both the coefficients have a ratio of 1 and 3.

Here, each spin orientation corresponds to its momentum. This type of orientation is the essence of spintronics devices. If all the electrons had oriented in one direction, then it would have behaved as a ferromagnetic. So, how does the spin-orbit coupling affect Gilbert damping? We have a processing magnetisation as shown in 1.1 irradiated by microwave radiation. This precessing magnetisation loses its angular momentum and falls back on its axis. This loss in angular momentum is transferred in the form of spin current to the 2DEG, where it absorbs the spin current due to the SOC effect. This loss of angular momentum is actually due to what we are calling Gilbert damping. The higher the damping higher the loss of angular momentum, and the higher is spin current generation. The loss of angular momentum is compensated by the ferromagnetic resonance. Now plotting the $\delta \alpha G_1$, $\delta \alpha G_2$ and $\delta \alpha G_3$ on matlab. We got curves with Gilbert damping and a given microwave frequency corresponding to the $\frac{\alpha}{\beta}=1$ and $\frac{\alpha}{\beta}=3$. for $\frac{\Gamma}{\Delta_0}=0.5$.

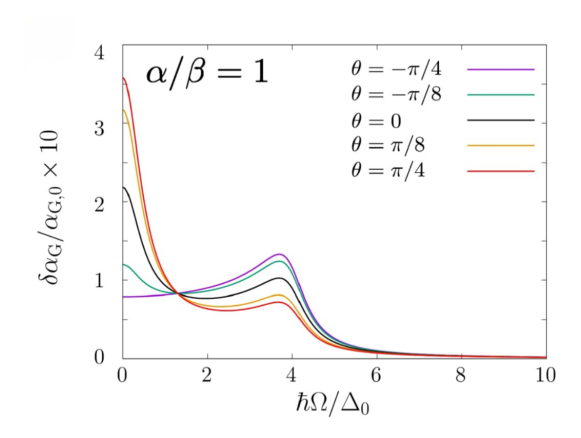


Figure 2.3: The increment in Gilbert damping, $\delta \alpha_G$ in 2DEG with FMR resonance frequency for $\frac{\alpha}{\beta} = 1$.

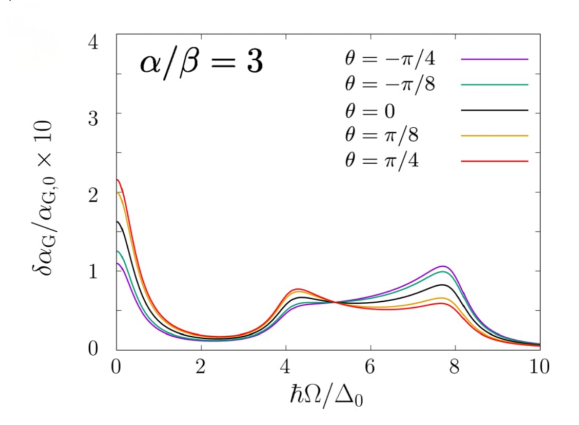


Figure 2.4: The increment in Gilbert damping, $\delta\alpha_G$ in 2DEG with FMR resonance frequency for $\frac{\alpha}{\beta}=3$.

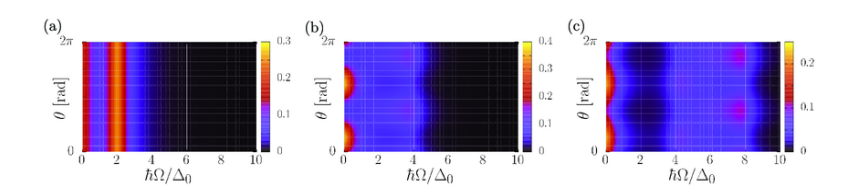


Figure 2.5: The contour plot for frequency vs Gilbert Damping.

We can see that $\delta \alpha_G$ relies on the resonance frequency, in comparison with the intrinsic damping factor for the bulk FI, α_G . In either of the cases, the increment explicitly relies on the alignment of spins in the FI. We got the peak at $\Omega = 0$ due to the part $\delta \alpha G_1$ and described by the second term in the Gilbert damping. As we increase our FMR frequency Ω , we get the broad peak shown by $\delta \alpha G_2$ due to the variation in the energy splitting as the magnon starts absorbing the energy. These magnons from the ferromagnetic insulator get absorbed by the 2DEG.

The range of $2h_{\text{eff}}$ is obtained from equation $|h_{\text{eff}}(\varphi)| \simeq k_F \sqrt{\alpha^2 + \beta^2 + 2\alpha\beta\sin(2\varphi)}$. Minimum value at $\theta = \frac{\pi}{4}$ and maximum value at $\theta = \frac{\pi}{4}$. For $\frac{\alpha}{\beta} = 1$, $0 \le 2h_{\text{eff}} \le 4\Delta_0$ and for $\frac{\alpha}{\beta} = 3$, we got $4\Delta_0 \le 2h_{\text{eff}} \le 8\Delta_0$. The physical reason behind getting a peak at $\Omega = 0$ in both cases is elastic spin-flip processes, which are independent of the frequency and depend on the alignment of the 2DEG effective field and the magnetisation direction of the ferromagnetic insulator. So, in the presence of magnetisation precession, the h_{eff} leads to energy dissipation. The broader peak shifts towards the higher frequency due to the higher Rashba coefficient, which causes higher spin splitting. So high frequency is required to match the energy gap between the splitting.

Chapter 3

Spin pumping via a 2D Heavy Hole Gas

We have considered the Gilbert damping for 2DEG and have seen the Rashba effect (arising due to SIA) in the enhancement of Gilbert damping. Now we considered a system of 2DHG and have checked the efficiency of these two. We use the same methodology to check the increase in GD at the 2DHG and the FI interface. 2DHG results from the same system, which changed the doping concentration in the AlGaAs and GaAs layers in semiconductor heterostructures. In 2DEG, we had a linear wave vector, while in the case of 2DHG, we have a wave vector in cubic form, which contributes to cubic Rashba SOC. The high role to damping increment comes from interband transitions, which show conductivitytype characteristics as the temperature goes to 0. We have checked the damping stays more in 2DHG because of the stronger effect of cubic Rashba SOC(A relativistic effect that combines the electron/holes motion to its spin)[3]. The interaction between Rashba SOC and magnon absorption in a 2D gas widens the optical response, with the shift in damping peak further at higher temperatures. Due to the strong Rashba effect, the spin wave interacting phase space increases, and we get a broad damping spectrum. Spin imbalance is sustained at the Fermi level, while a zero Fermi level suppresses it. The Rashba effect is

tunable and can be tuned with an external electric field.

In the next chapter, we will explore the same spin pumping framework in 2DHG.

3.1 2DHG's Introduction

The correlation between spin-orbit interactions and magnetisation dynamics at the junction of 2DHGs and FIs, with particular emphasis on SOC effects in 2DHGs emerging at p-type Al/GaAs interfaces. It plays an important role in spin transport (Spin transport moves spins without necessarily moving charge → Creates spin currents) and magnetic effects arising from the p-orbital properties of charge carriers (Unlike s-orbital electrons, which have negligible SOC. p-orbitals have intrinsic angular momentum that is l = 1, which leads to strong SOC effects. It means spin and momentum are strongly coupled, which modifies how spins are transported in the system. In 2DHGs, the stronger SOC relative to 2DEGs gives rise to a specific magnetic phenomenon when interfaced with a ferromagnetic insulator. At this interface, the exchange interaction between spin-polarised electrons from the ferromagnetic material and Rashba spin-orbitcoupled holes in the 2DHG gives rise to special magnetic behaviour, which plays a key role in diverse spintronics applications. One significant outcome of this exchange interaction will be enhanced GD, which governs energy loss in magnetisation. Cubic Rashba SOC, which is strong in 2DHG/FI heterostructures, helps effective spin dissipation, which enhances even more damping. At the junction, strong spin-orbit coupling enhances spin transfer, which leads to effective angular momentum loss. The interplay between SOC-induced spin relaxation and spin-pumping introduces an efficient mechanism for regulating magnetisation processes, which makes these structures a strong entity for spintronic implementations that demand quick and energy-optimised magnetic switching. Continued groundbreaking studies have investigated different faces of spin-pumping in depth, which makes significant contributions to our work.

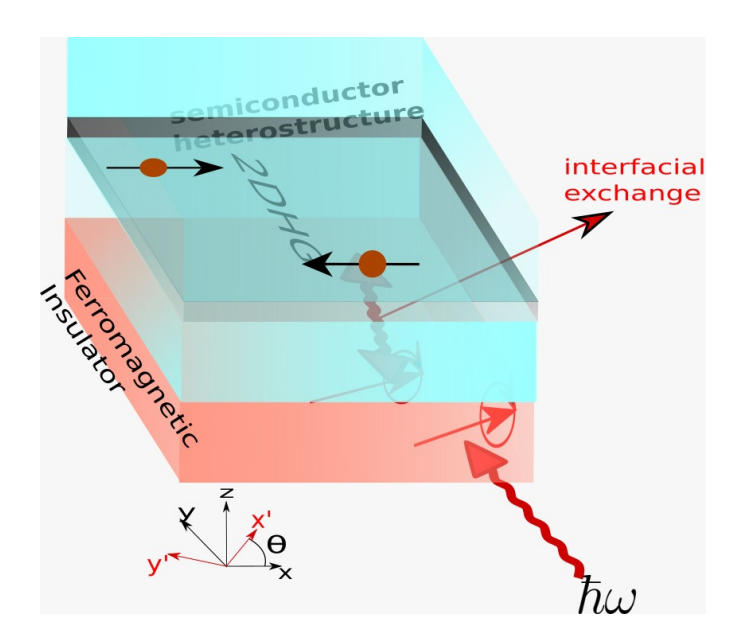


Figure 3.1: Schematic of our system with a ferromagnetic layer irradiated with microwave frequency, in junction with 2DHG in semiconductor heterostructure.

We tried to show that this increase in Gilbert damping is mainly influenced by transitions between the interband energy levels that exhibit resemblance to conductivity in lower temperature conditions. At higher temperatures, spin wave behaves dominantly, causing an expansion of the spectrum and a thermalbased alteration in the peak of the damping spectrum, which eventually leads to angular momentum flow by the spin injection mechanism. Additionally, I tried to find the optical spectrum that is suitable for microwave irradiation, optimising spin injection process efficiency and precise damping control. These things emphasise the important role of the Fermi level energy in maintaining spin non-uniformity and facilitating spin current injection. Noting that, putting $E_f = 0$ in a 2DHG suppresses the phenomenon, which is just the opposite of the 2DEG. We also find that strong Rashba spin-orbit coupling increases spin-wave interactions and expands the frequency-dependent behaviour by shortening spinwave relaxation time due to enhanced dispersion, as a result of which the energy dissipation enhances across an extended frequency spectrum. Remarkably, the quality of changing tuning of RSOC strength in 2DHGs through the applied

electric field helps instantaneous regulation of spin current loss. The insights put 2DHG based heterostructures as an important platform for electrically tunable spintronics, paving the way for new aspects of high-efficiency spin dynamics for advanced applications.

3.2 Composite system Hamiltonian

The total Hamiltonian H_{tot} of the composite system comprises three parts,

$$H_{\text{tot}} = H_{\text{2DHG}} + H_{\text{FI}} + H_{\text{ex}}.$$

Each of these illustrates a unique aspect of the system's physical interactions.

3.3 Two-Dimensional Heavy Hole Gas

We can write Hamiltonian general representation, $H_{\rm 2DHG}$, for a 2DHG with k cubic SOC, in the framework of creation and annihilation operator representation for spin pointing up $(c_{k,\uparrow}^{\dagger}, c_{k,\uparrow})$ and spin pointing down $(c_{k,\downarrow}^{\dagger}, c_{k,\downarrow})$ holes in k space. We write the energy operator for the system, which has cubic Rashba and Dresselhaus SOC, as [7]

$$H_{\text{2DHG}} = \sum_{k} \begin{pmatrix} c_{k,\uparrow}^{\dagger} & c_{k,\downarrow}^{\dagger} \end{pmatrix} H_{\text{2DHG}}(k) \begin{pmatrix} c_{k,\uparrow} \\ c_{k,\downarrow} \end{pmatrix}$$
(3.1)

Here, H_{2DHG} gives the effective Hamiltonian for SOC 2DHG of wave vector k, and it has both the Rashba and Dresselhaus SOC given below[7]

$$H_{\text{2DHG}}(k) = \left[\zeta(k) - E_f\right] \sigma_0 + i\alpha \frac{1}{2} (k_-^3 \sigma_- - k_+^3 \sigma_+) - \frac{\beta}{2} (k_- k_+ k_- \sigma_+ + k_+ k_- k_+ \sigma_-), (3.2)$$

Here, $k_{\pm} = k_x \pm i k_y$ are the complex wave vector components, and $\frac{\sigma_{+}}{\sigma_{-}}$ are the spin-creation/annihilation operators. The initial term is the hole's kinetic en-

ergy, with $\zeta(k) = \frac{2k^2}{2m}$ is the free motion of mass m energy and the Fermi state ${}^{\prime}E_f{}^{\prime}$. The other two terms describe the Dresselhaus SOC and Rashba SOC, respectively, where α and β are the coupling constants that direct the intensity of interplay. The cubic wave vector is due to the p orbitals. The interplay plays an important role in directing spin dissipation processes, magnetisation dynamics and spin-momentum locking in 2DHG systems, which directly affects the spin pumping efficacy from a ferromagnetic insulator into the 2DHG. This is a central point of our thesis. We can write the strength of SOC in 2DHG as-

$$|h_{SOC}(k)| = k^3 \Delta(\phi), \tag{3.3}$$

where
$$\Delta(\phi)$$

$$\Delta(\phi) = \sqrt{\alpha^2 + \beta^2 - 2\alpha\beta\sin(2\phi)}, \tag{3.4}$$

 ϕ is the azimuthal angle in phase space. This shows that the strength of SOC also depends on the azimuthal angle ϕ .

$$h_{\text{SOC}}(k) = \begin{pmatrix} h_x \\ h_y \\ 0 \end{pmatrix} = \begin{pmatrix} k^3(-\alpha \sin 3\phi + \beta \cos \phi) \\ k^3(\alpha \sin 3\phi + \beta \cos \phi) \\ 0 \end{pmatrix}. \tag{3.5}$$

The SOC field components are projected onto the xy plane in k space, and their relationship with ϕ shows an intricate, angle-based spin configuration. The terms $\sin(3\phi)$ and $\cos(3\phi)$ relates Dresselhaus SOC and the Rashba SOC interplay, and both have different uniformity in the k space. Now, the system's energy can be written as $E_s(k)$

$$E_s(k) = \zeta(k) + s|h_{SOC}(k)|, \qquad (3.6)$$

Here 's' denotes the spin configuration, and the other term, $s|h_{SOC}(k)|$, with $s = \pm$. describes the shift in energy to the entire system due to the SOC. We now

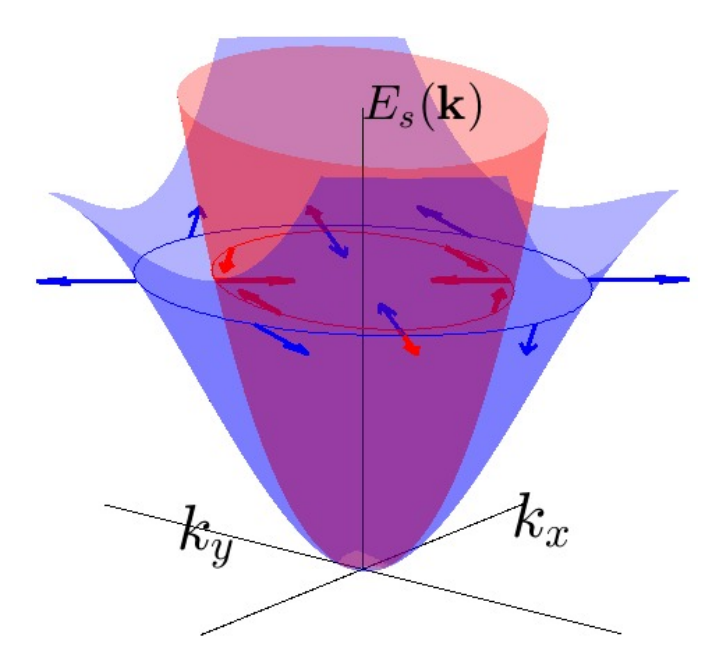


Figure 3.2: Energy dispersion $E_s(k)$ due to SOC, in which the pink part represents the s=+1 and the other colour represents to s=-1. Arrows represent the spin configuration along the Fermi contours, which shows the opposing chirality of the two parts. The parameters are chosen such that the ratio of spin-orbit coupling strengths is $\alpha/\beta=2$.

consider the retarded Green's function for a 2DHG-

$$[E - H_{2DHG}(r)]G_0(r, r') = \delta(r - r'),$$
 (3.7)

where $G_0(r,r')$ shows the Green's function of the clean system under consideration. This Green's function is invariant under symmetry and satisfies $G_0(r;r') = G_0(r';r)$. The energy operator of the setup is changed, including scattering due to impurities, expressed as $H'_{2DHG} = H_{2DHG} + V_{\text{imp}}$. The impurity potential V_{imp} is modeled as-

$$V_{\text{imp}} = u \sum_{i \in \text{imp}} \sum_{\sigma} \Psi^{\dagger}(R_i) \Psi(R_i), \qquad (3.8)$$

We can write the Green's function from the time domain to the frequency domain as

$$G(k, i\omega_n) = \hbar\beta \int_0^\beta d\tau \, e^{i\omega_n \tau} G(k, \tau). \tag{3.9}$$

The Green's function of the pure system in Matsubara frequencies is

$$G_0(k, i\omega_m) = \frac{(i\hbar\omega_m - \zeta(k))\sigma_0 - h_{SOC} \cdot \sigma}{(i\hbar\omega_m - E_+(k))(i\hbar\omega_m - E_-(k))}.$$
(3.10)

The Green's function after impurity broadening is given by

$$G(k, i\omega_m) = \frac{\left[(i\hbar\omega_m - \zeta(k) + i\Gamma/2\operatorname{sgn}(\omega_m))\sigma_0 - h_{\text{SOC}} \cdot \sigma \right]}{\prod_{s=\pm} \left[(i\hbar\omega_m - E_s(k) + i\Gamma/2\operatorname{sgn}(\omega_m)) \right]}.$$
 (3.11)

where $i\omega_m$ is the Matsubara frequency of fermions and Γ represents the broadening of the peak due to the possible impurities.

3.4 Ferromagnetic Insulator

Ferromagnetic insulators have a strong exchange interaction, which creates a net magnetisation in them. In FI, quantised spin waves (magnons) serve as the spin magnetic moment carrier, enabling spin transport independent of charge transport. Localised spins of ions or atoms are usually responsible for the magnetic moments, which is different from the case of metals. In FI, we can represent the spin vector by S_l at each lattice site l. Writing the mean value of this spin vector in spherical coordinates.

$$\langle S_l \rangle = (\langle S_x \rangle_l, \langle S_y \rangle_l, \langle S_z \rangle_l)' = S_0 m,$$
 (3.12)

Where S_0 is the magnitude of the spin, $\mathbf{m} = (\cos \theta, \sin \theta, 0)$ and θ is the angle made with reference axis. For relating new coordinates to the old coordinates.

$$\begin{pmatrix}
S_{x'} \\
S_{y'} \\
S_{z'}
\end{pmatrix} = R(\theta, \phi) \begin{pmatrix}
S_x \\
S_y \\
S_z
\end{pmatrix}.$$
(3.13)

The components of spin in terms of bosonic raising (b_l^{\dagger}) and lowering (b_l) operator are-

$$S_l^+ = S_{y'}^l + iS_{z'}^l = \sqrt{2S_0} \left(1 - \frac{b_l^{\dagger} b_l}{2S} \right)^{\frac{1}{2}} b_l, \tag{3.14}$$

$$S_l^- = b_l^{\dagger} \sqrt{2S_0} \left(1 - \frac{b_l^{\dagger} b_l}{2S} \right)^{\frac{1}{2}}, \tag{3.15}$$

$$S_{x'}^l = S_0 - b_l^{\dagger} b_l. \tag{3.16}$$

here S_l^+ and S_l^- are spin raising and spin lowering operator. $S_l^{x'}$ is the longitudinal component of the spin. So, now Hamiltonian can be written as [7]

$$H_{\rm FI} = -J \sum_{\langle l, m \rangle} S_l \cdot S_m - g\mu_B h_{\rm dc} \sum_l S_{x'}^l. \tag{3.17}$$

The first term of the Hamiltonian represents the spin-spin exchange between the neighbouring spins, while the other term is due to Zeeman splitting caused by the applied DC magnetic field (h_{dc}) . Its Hamiltonian can be rewritten using the Fourier transform, which is given by

$$H_{\rm FI} = \sum_{q} \hbar \omega_q b_q^{\dagger} b_q, \tag{3.18}$$

Here,

$$\hbar\omega_q = D|q|^2 + g\mu_B h_{\rm dc}.$$
 (3.19)

We write the Green's function at q = 0 in the frequency domain

$$G(q=0,\omega) \approx \frac{2S_0/\hbar}{\omega - \omega_{q=0} + i[\alpha_G + \delta\alpha_G(\omega, T)]\omega}.$$
 (3.20)

This will be used while dealing with the combination of FI and 2DHG at the interface.

3.5 Interfacial Exchange Interaction

In this section, we studied the interaction that takes place between the ferromagnetic insulator and the 2DHG. This is mediated by exchange interaction. This is the desired interaction and helps us study the system's net magnetic characteristics. We describe the Hamiltonian of interfacial exchange interaction through the interaction between 2DHG spins and ferromagnetic insulator spins.

$$\begin{pmatrix} s_{x'} \\ s_{y'} \\ s_{z'} \end{pmatrix} = R(\theta, \phi) \begin{pmatrix} s_x \\ s_y \\ s_z \end{pmatrix}.$$
 The operator s_k^a (where $a = x, y, z$), to be written in the

creation and annihilation operator (c_q^{\dagger}, σ) and (c_{k+q}, σ) as

$$s_k^a = \sum_{\sigma\sigma'} \sum_q c_{q,\sigma}^{\dagger}(\sigma^a)_{\sigma\sigma'} c_{k+q,\sigma'}. \tag{3.21}$$

Here, the Pauli matrix (σ_a) is the mediator between the two. We can now define the flip of spin state operators in the rotated coordinate system as

$$s_{k,+}^{x'} = s_k^{y'} + is_k^{z'}, (3.22)$$

$$s_{k,-}^{x'} = (s_{k,+}^{x'})^{\dagger}.$$
 (3.23)

In the next section, we tried to calculate the Gibert damping.

3.6 Gilbert Damping Calculation

We applied the Green's function framework to explore spin pumping, It gives us a strong method for showing spin kinematics and the eventual increment in the Gilbert damping factor. Here, we will evaluate the refinement of the Gilbert damping term because of exchange interactions at the interface in 2DHG in junction with FI. The exchange interaction at the interface changes the electronic structure by adding an impurity potential, due to which correction in

self-energy are done. [7]

$$\Sigma(k, i\omega_n) = \frac{|T_1|^2}{4\beta} \sum_{k', i\omega_m} \text{Tr} \left[\sigma_{x'}^- G(k', i\omega_m) \sigma_{x'}^+ G(k' + k, i\omega_m + i\omega_n) \right]$$
(3.24)

These corrections account for scattering and spin flipping. Due to SOC in the 2DHG, scattering depending on spin is further increased, spin-dependent, and it greatly influences magnetisation dynamics. To study these outcomes, we are using the Green's function within the framework of the second-order perturbation domain as given below.[7]

$$G(k, i\omega_m) = \frac{1}{\left[G_0(k, i\omega_m)\right]^{-1} - \Sigma(k, i\omega_m)}$$
(3.25)

Here, $G_0(k, i\omega_m)$ is the Green function and $\Sigma(k, i\omega_m)$ is the self energy term. The imaginary part self-energy describes the widening of energy states because of fluctuations in the spin, which explicitly affect the loss of magnetisation dynamics[6]. This change leads to an increase in the Gilbert damping constant($\delta\alpha_G(\omega, T)$). This self-energy includes spin interactions, and spin reversal scattering is given by [7]

$$\Sigma(k, i\omega_n) = \frac{|T_1|^2}{4\beta} \sum_{k', i\omega_m} \text{Tr} \left[\sigma_{x'}^- G(k', i\omega_m) \sigma_{x'}^+ G(k' + k, i\omega_m + i\omega_n) \right]$$
(3.26)

The Green's function in k-space of the Matsubara frequency $i\omega_m$ is of the form,

$$G(k, i\omega_m) = \frac{A(k, i\omega_m) \,\sigma_0 - \mathbf{h}_{SOC} \cdot \boldsymbol{\sigma}}{B(k, i\omega_m)}$$
(3.27)

 h_{SOC} and σ is the dot product of the spin-orbit field and Pauli matrices. Here

$$A(k, i\omega_m) = i\hbar\omega_m - \zeta(k) + i\frac{\Gamma}{2}\operatorname{sgn}(\omega_m)$$
(3.28)

and

$$B(k, i\omega_m) = \prod_{s=+} \left(i\hbar\omega_m - E_s(k) + i\frac{\Gamma}{2}\operatorname{sgn}(\omega_m) \right)$$
 (3.29)

The self-energy term can be given as

$$\Sigma\left(\mathbf{q}=0,i\omega_{m}\right)=\frac{\left|\mathcal{T}_{1}\right|^{2}}{\beta}\sum_{k,i\omega_{m}}\frac{\mathcal{A}\left(\mathbf{k},i\omega_{m}\right)-\hat{\mathbf{h}}_{SOC}\cdot\mathbf{m}}{\mathcal{B}\left(\mathbf{k},i\omega_{m}\right)}\frac{\mathcal{A}\left(\mathbf{k}+\mathbf{k}',i\left(\omega_{m}+\omega_{n}\right)\right)+\hat{\mathbf{h}}_{SOC}\cdot\mathbf{m}}{\mathcal{B}\left(\mathbf{k}+\mathbf{k}',i\left(\omega_{m}+\omega_{n}\right)\right)}$$

3.7 Result of 2D Heavy Hole Gas

The final equation we arrived at is

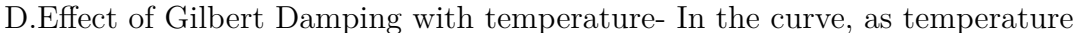
$$\frac{\delta \alpha_G(\omega, T)}{\alpha_{G,0}} = -\sum_{s,s'=\pm 1} \int_0^\infty d\xi \int_0^{2\pi} \frac{d\phi}{2\pi} \delta_L \left[\hbar \omega + (s - s') |\mathbf{h}_{SOC}(\mathbf{k})| \right] \\
\times \left[\frac{1 - s \hat{\mathbf{h}}_{SOC}(\mathbf{k}) \cdot \mathbf{m}}{2} \cdot \frac{1 + s' \hat{\mathbf{h}}_{SOC}(\mathbf{k})}{2} \right]$$
(3.30)

A. Switching from states s = -1 and s' = 1

At larger frequencies, the transitions in distinct energy levels (interband) become largely dominating as the optical energy is sufficient to stimulate the spin to the energy level. The useful shifts adding to the optical feedback are between states s = -1 and s' = 1, as these belong to the different spin flips while interacting with the EM field. These shifts are directed through the energy differences $\hbar\omega + (s - s') |h_{\rm SOC}|$. This electron excitation term verifies that the dynamics of spin-switching are appropriately incorporated in the model, significantly influencing the frequency-dependent optical response.

B. Inter-band versus Intra-band Transitions: The transitions within and between bands' behaviour is determined by the SOC and the dispersion of energy. The term $\hat{h}_{\text{SOC}}(\mathbf{k}) \cdot \mathbf{m}$ changes the intensity of these shifts. At lower frequency, the transitions within the bands are strong since the energy needed for intraband transitions is low. This is shown by the lower energy scale $\hbar\omega$ involved in the shift.

C. Optical Transitions: In our study, photon-driven transition happens in the frequency spectrum of microwave $\hbar\omega_2 \leq \hbar\omega \leq \hbar\omega_1$ while $k_f^-(\phi)$ and $k_f^+(\phi)$ are Fermi momentum vectors for different spin sub-levels. We have analysed that within this range a dominating increment in Gilbert damping factor happens because of the presence of van-hove singularities. These singularity clearly shows the conductance-like optical transition, especially while the widening parameter $\Gamma \to 0$, results in a peak directly at one of the key transition frequencies.



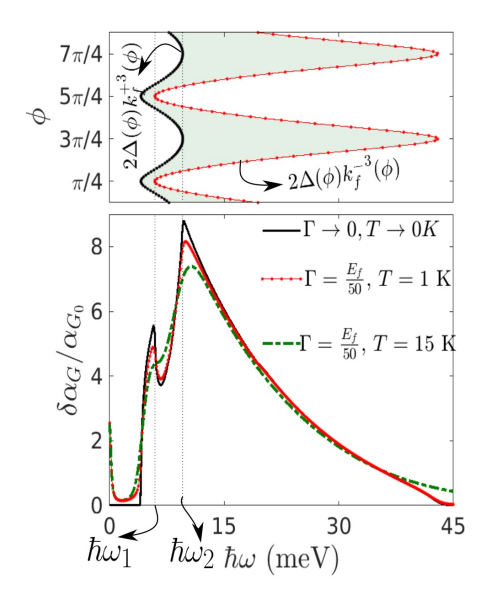


Figure 3.3: variation in the δ with frequencies **k**.

increases, the damping width also increases, indicating enhanced angular momentum absorption from the ferromagnetic insulator. This behaviour arises due to increased thermal occupation of states near the Fermi level, which opens up more ways for spin-flip transitions and interband scattering. Additionally, higher temperature broadens the magnon energy distribution, increasing the overlap with hole states, which in turn strengthens the spin pumping efficiency. The particular transition frequency where the singularities arise is given by these

conditions-

$$\hbar\omega = \begin{cases} \hbar\omega_1, & \text{if } \phi = \frac{\pi}{4}, \frac{5\pi}{4} \\ \hbar\omega_2, & \text{if } \phi = \frac{3\pi}{4}, \frac{7\pi}{4} \end{cases}$$

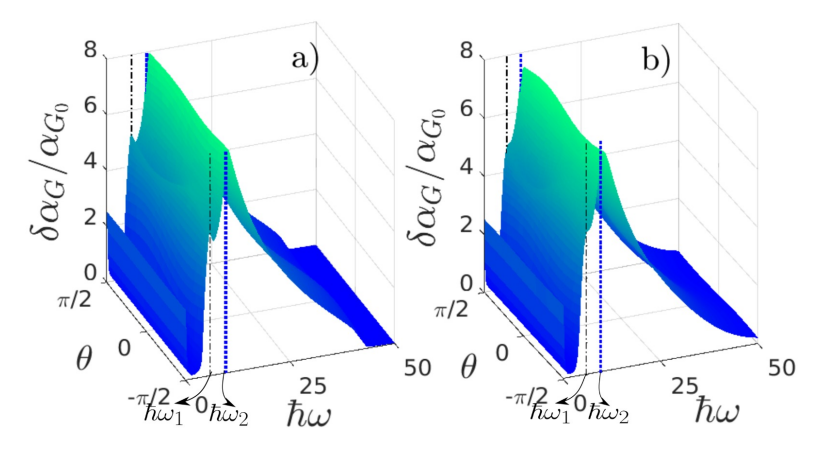


Figure 3.4: Schematic of contour plot at range of frequencies frequencies δ vs ω .

3.8 Enhancement of Gilbert Damping

Practically, it says that at these particular microwave frequencies and azimuthal angular configurations, the states that are available for transition are maximised, which leads to an increase in the Gilbert factor parameter. Concerning spin pumping, it explicitly affects the spin current production by changing the absorption behaviour that depends on the Rashba SOC amplitude α [4]. These irregularities show a crucial thing in the density of states where the transition probability is significant. The lifetime of spin wave τ explains the time period during which a spin wave stays coherent before decaying because of interaction. A short spin wave lifetime leads to enhanced spectral widening. In this case, the widening is affected by the cubic Spin-Orbit Coupling and the exchange coupling at the interface, which affects the increment in the Gilbert factor.

1. Role of the Fermi level-

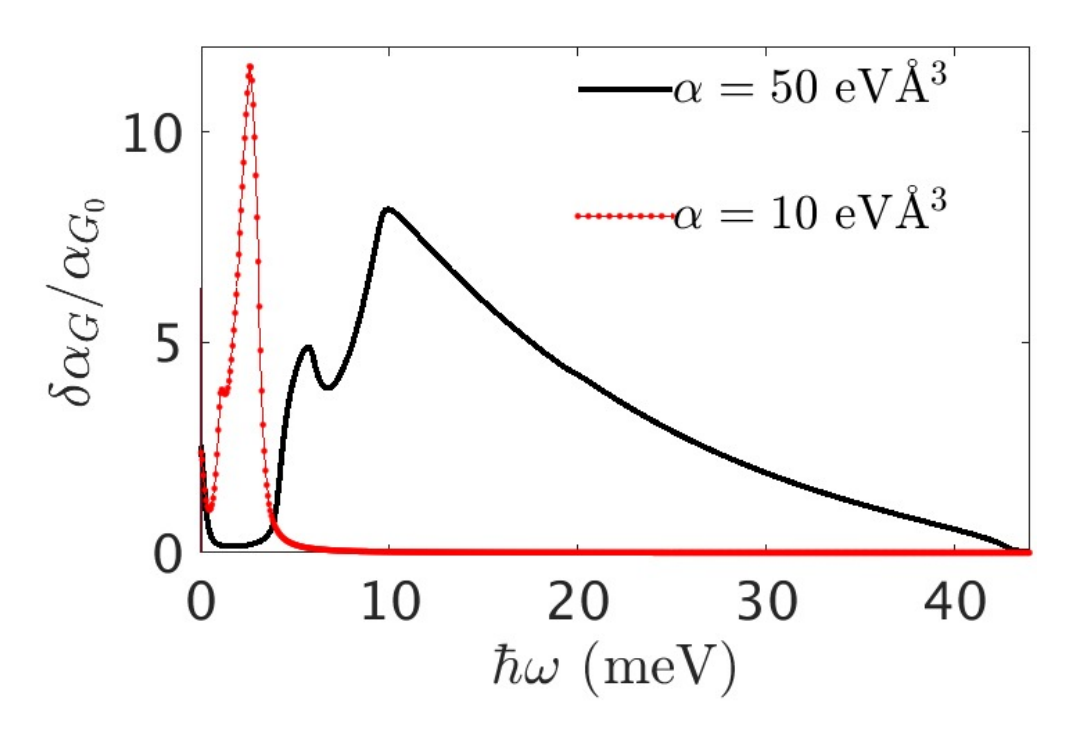


Figure 3.5: The curve showing enhancement of Gilbert damping vs frequency at different values of Rashba coefficient α .

In addition to this, the position of the Fermi energy state E_f directs the spin imbalances by making an unequal spin population in the up and down spin levels. A non-zero Fermi value confirms a definite spin current, as putting $E_f = 0$ removes the spin imbalance, thereby damping the spin flow. If the Fermi energy = 0, it expresses the absence of spin polarisation in up and down spin holes, which results in no net spin accumulation and no spin current absorbed by the other layer material. Non-magnetic material eliminates the spin differences. When there is no spin accumulation, the main force for spin transport from the ferromagnetic insulator quashes, which leads to a decrease in the Gilbert damping. This effect differentiates the 2DHG system from a usual 2DEG, where spin differences and related spin currents occur distinctly. In this system, the complex dependence on spin accumulation shows its clear dynamics.

2. Effect of Rashba SOC on spectrum widening and Gilbert damping Increment-

We can see that a strong Rashba SOC affects the spectrum widening of the

Gilbert factor. This happens due to the RSOC changes the scattering of the spin waves by widening the phase space for spin wave interaction and by decreasing the spin wave relaxation time. As the Rashba SOC increases, the widening of the spectral function also enhances, which allows the Gilbert factor to spread over a wide range of frequencies. As a result, the spin angular moment loss becomes more significant over a large band of frequencies.

Chapter 4

Summary

We studied the spin pumping in a system aided by 2DEG and 2DHG, which occurs in n-doped and p-doped AlGaAs/GaAs heterostructures, respectively. The increment in the Gilbert damping, which happens due to the back action of angular momentum injected into the 2DEG/2DHG. Higher Rashba effect causes higher spin current to get absorbed by the 2DEG, which in turn causes a high rate of change of magnetisation in the FI. The angular momentum lost in the form of spin current again gets excited by the FMR frequency. The high value of Rashba effects requires a high Resonant frequency to show the broad peak. We used the Hamiltonian of the 2DEG and FI, used the Green function and then studied their combined effect at interface using the second-order perturbation. In the 2DHG system, we studied this phenomenon which is cubic in momentum. In summary, our study marks the important role of cubic Rashba SOC in increasing the Gilbert damping factor where the 2DHG acts as the spin absorbing layer for spin pumping action in the FI. The presence of cubic Rashba SOC eases smooth spin-orbit scattering, enhancing spin-pumping efficiency in comparison to our earlier 2DEG system and increasing angular momentum abosorption[2]. Our findings show that the interplay between Rashba SOC and magnon absorption takes to spectral widening, changing dynamics of spin relaxation and altering the characteristic frequency associated with the damping

peak[5]. The main contribution to the Gilbert factor comes from interband excitations, expected to show conductance-like properties in the limit of gamma tends to zero. We showed that RSOC strength can be changed through an external electric field. This straightforwardly influences the amplitude of the Gilbert damping factor. Higher field increases Rashba SOC, promoting enhanced spin loss and more effective transfer of spin angular momentum, while a lower field decreases SOC, reducing damping. This tunability offers a promising route for designing energy-efficient spintronic systems. Additionally, our study emphasises the importance of a finite Fermi energy level in keeping spin imbalance, which is crucial for spin transport and dissipation. Keeping the Fermi energy level to zero eliminates spin differences and weakens damping and emphasises the basic link between spin pumping and the Fermi state. These observations show the possibility for tunable spin dynamics through electric potential in heterostructures.

Bibliography

- Yama, M., Tatsuno, M., Kato, T., & Matsuo, M. Spin pumping of twodimensional electron gas with Rashba and Dresselhaus spin-orbit interactions, Phys. Rev. B. 104, 054410 (2021)
- [2] Zarea, M., & Ulloa, S. E. Spin Hall effect in two-dimensional p-type semiconductors in a magnetic field. Phys. Rev. **73**, 165306 (2006)
- [3] Nichele, F., Chesi, S., Hennel, S., Wittmann, A., Gerl, C., Wegscheider, W., Loss, D., Ihn, T., & Ensslin, K. Characterisation of Spin-Orbit Interactions of GaAs Heavy Holes Using a Quantum Point Contact. Phys. Rev. 113 046801 (2014)
- [4] Rojas Sánchez, J.C., Vila, L., Desfonds, G., Gambarelli, S., Attané, J.P., De Teresa, J.M., Magén, C., & Fert, A. Spin-to-charge conversion using Rashba coupling at the interface between non-magnetic materials, Nat. Com, 4, 2944 (2013).
- [5] Bulaev, D. V., & Loss, D. Spin Relaxation and Decoherence of Holes in Quantum Dots. Phys. Rev. **95**, 076805 (2004)
- [6] Hannay, J. D. Computational simulations of thermally activated magnetisation dynamics at high frequencies. (2001)
- [7] Mawrie A, Saha S, Enhanced gilbert damping via cubic spin-Orbit coupling at 2DHG/ferromagnetic insulator interface (2025).